Discover Oncology

Analysis

Construction of a novel CD8T cell-related index for predicting clinical outcomes and immune landscape in ovarian cancer by combined single-cell and RNA-sequencing analysis

Yu Zhang[1,2] · **Peng Wan**[1,2] · **Liangliang Wang**[1,2] · **Ruiping Ren**[1,2]

Received: 6 October 2024 / Accepted: 5 May 2025
Published online: 12 May 2025

Abstract

Background CD8T cells, also known as cytotoxic T lymphocytes, play a key role in the tumor immune microenvironment (TME) and immune response. The aim of this study was to explore the potential role of CD8T cell-associated biomarkers in predicting prognosis and immunotherapy efficacy in ovarian cancer.

Methods The single-cell sequencing data from the EMTAB8107 cohort were used to identify CD8 T-cell subtypes. The TCGA-OV cohort was involved in constructing a machine learning-based CD8T cell-associated index (CCAI). Additionally, independent ovarian cancer cohorts GSE26712 and GSE26193 were used to validate the predictive validity of CCAI. Multifactorial Cox regression and ROC analysis were applied to assess CCAI. The STRING database was used to clarify the interactions of CD8 T-cell-associated molecules. Furthermore, immune landscape analysis was performed using CIBERSORT, ssGSEA, TIMER, and ESTIMATE algorithms. Tumor mutation burden (TMB) analysis and drug sensitivity analysis were used to evaluate the potential predictive value of CCAI.

Results The CCAI, comprising LRP1, PLAUR, OGN, TAP1, ISG20, CXCR4, IL2RG, LCK, and CD3G, serves as a reliable prognostic marker for ovarian cancer patients, demonstrating robust predictive accuracy across various patient cohorts. Notably, individuals with low CCAI tend to exhibit immunoinflammatory tumor characteristics.

Conclusions The developed CCAI serves as a promising prognostic biomarker for ovarian cancer, accurately predicting patient outcomes. Additionally, it differentiates between patients with distinct immune landscape profiles. This insight enables personalized treatment strategies and facilitates the exploration of underlying mechanisms involving CCAI-related molecules.

Keywords Ovarian cancer · CD8T · Single-cell RNA · Prognosis · Immune microenvironment

Supplementary Information The online version contains supplementary material available at https://doi.org/10.1007/s12672-025-02582-4.

✉ Yu Zhang, rmzhangyu11518@nbu.edu.cn; Peng Wan, 526079589@qq.com; Liangliang Wang, Ww1321467606@163.com; Ruiping Ren, 15967481@qq.com | [1]Department of Chemoradiotherapy, The Affiliated People's Hospital of Ningbo University, Ningbo, China. [2]Chemoradiotherapy Center of Oncology, The Affifiliated People's Hospital of Ningbo University, Ningbo, China.

1 Introduction

Ovarian cancer (OC) ranks third among gynecological cancers, following cervical and uterine corpus cancers, yet it has the second highest mortality rate [1]. While early-stage cases generally have a favorable prognosis, most patients are diagnosed in advanced stages [2, 3]. Although many patients achieve remission with surgery and platinum-based chemotherapy, a significant number die due to platinum resistance and disease progression, with a 5-year survival rate of less than 50% [4]. Unfortunately, reliable biomarkers for predicting ovarian cancer prognosis are still lacking. Therefore, there is an urgent need to identify more informative diagnostic and prognostic factors for OC.

Emerging evidence suggests that OC is immunogenic, making it susceptible to recognition by the host immune system [5]. The dynamic interaction between the immune system and cancer cells plays a pivotal role in tumor progression. As a result, significant efforts have been directed toward identifying and characterizing tumor infiltrating lymphocytes (TILs) in ovarian cancer over recent years [6, 7]. CD8 T cells, also known as cytotoxic T lymphocytes, are a crucial subtype of TILs integral to the immune response [8, 9]. Their interaction with antigen-presenting cells involves recognizing and binding to major histocompatibility complex I molecules, leading to the activation of CD8 T cells [10, 11]. CD8 T lymphocytes have the ability to kill OC cells in tumour immune microenvironment (TIME), and their infiltration levels correlate with patient survival [12]. Furthermore, CD8T cells interact with tumor cells and other TILs in the TIME, influencing cancer evolution and the efficacy of anti-tumor drugs [13]. Understanding the unique role of CD8 T cells in evaluating outcomes and immune landscape in OC is crucial for uncovering reliable predictive biomarkers.

Recent advancements in high-throughput sequencing data across diverse cancers, combined with the evolution of bioinformatics technologies, have greatly facilitated the identification of crucial targets and novel predictive biomarkers [14–16]. In this study, we conducted a comprehensive analysis of CD8 T cell-associated prognostic markers to predict OC clinical outcomes and immune landscape. Our findings provide valuable insights into the potential roles of CD8 T cell-related molecules in OC progression and immune regulation.

2 Materials and methods

2.1 Data sources

Transcriptome datasets, nucleotide variation data, and corresponding clinical information for patients with ovarian cancer were retrieved from the TCGA-OV cohort (https://portal.gdc.cancer.gov/repository). A total of 587 patients with both transcriptomic and survival data were included in the subsequent analysis, with their clinicopathological parameters summarized in Table 1. The ovarian cancer cohorts GSE26712 and GSE26193 from the GEO database (https://www.ncbi.nlm.nih.gov/) were utilized as validation cohorts. Single-cell sequencing data matrices and cell marker annotations for the EMTAB8107 cohort were retrieved from TISCH Dataset Browser (http://tisch.comp-genomics.org/) [17]. Immunohistochemical images of index-associated genes in OC tissues were extracted from the HPA database (https://www.proteinatlas.org) (Table S1) [18]. Tumor-infiltrating immune cells data were extracted from the TIMER platform (http://timer.comp-genomics.org/) [19], while immunological gene sets were acquired from the ImmPort Immunological Data Platform (https://www.immport.org/home) [20].

2.2 Extraction of CD8T cell-related differentially expressed genes

R (version 4.2.2) was employed to extract differentially expressed genes (DEGs) between CD8T cells in the EMTAB8107 cohort and other cells (Fold Change > 1.5, Adjusted-$P < 0.05$). The R packages "VennDiagram" and "ggplot2" were used to analyze the intersection of DEGs with immune-related genes and to construct a Venn diagram. The STRING Data Resource (https://cn.string-db.org/) was utilised to generate a network of interactions among the intersecting genes, and neighboring nodes were ranked based on their interactions.

Table 1 Clinicopathological indicators in TCGA-OV cohort

Clinicopathological indicators	Type	TCGA-OV cohort (n = 587)
Age	≤60	326 (55.54%)
	>60	261 (44.46%)
Grade	G1	6 (1.02%)
	G2	69 (11.76%)
	G3	495 (84.33%)
	Not available	17 (2.89%)
TNM-Stage	Stage I	17 (2.89%)
	Stage II	30 (5.11%)
	Stage III	446 (76.00%)
	Stage IV	89 (15.16%)
	Not available	5 (0.85%)
Survival status	Alive	236 (40.20%)
	Deceased	350 (59.62%)
	Not available	1 (0.17%)
Pathological type	Serous cystadenocarcinoma	578 (98.47%)
	Serous surface papillary carcinoma	2 (0.34%)
	Papillary serous cystadenocarcinoma	4 (0.68%)
	Not available	3 (0.51%)

2.3 Development of a CD8T cell associated index (CCAI) in OC

The R "limma" was used to merge transcriptomic and survival data for subsequent analyses. The "survival" and "survminer" packages were employed to perform univariate Cox regression, identifying DEGs associated with OC prognosis in the TCGA-OV cohort. Subsequently, the Least Absolute Shrinkage and Selection Operator (LASSO) was applied to shrink unimportant regression coefficients to zero, thereby excluding variables and selecting the DEGs for constructing the CCAI. The Kaplan-Meier (K-M) method was used to assess the impact of CCAI-related genes on ovarian cancer survival. CCAI scores for patients in the TCGA-OV cohort were calculated based on the regression coefficients and expression values of the DEGs in the CCAI. Finally, patients in TCGA cohort were classified into high- and low-CCAI subgroups based on the median CCAI score.

2.4 Verification and assessment of CCAI in OC

The K-M method was applied to the TCGA cohort for survival validation to determine survival differences in risk-stratified populations based on the CCAI. The "pheatmap" was used to visualize the expression of CCAI-associated genes in distinct risk subgroups. To further clarify the predictive validity of the CCAFI, the K-M method was also applied to survival analyses of the validation cohorts GSE26712 and GSE26193. Multivariate Cox regression was then utilised to assess the impact of the CCAI and key clinical parameters on ovarian cancer prognosis. Finally, receiver operating characteristic (ROC) analysis was conducted to evaluate the predictive stability of the CCAI, with the "tidyverse", "colorBrewer", "grid", and "ggplot2" packages employed for the ROC analysis and visualization of the curves.

2.5 Construction of a CCAI-based nomogram

Cox regression revealed that the CCAI and age were independent prognostic variables for OC. These two variables were then used to develop a nomogram to better predict patient clinical outcomes. The R packages "regplot", "rms" and "survival" were utilized for the development and visualization of the nomograms. Moreover, calibration curves were employed to assess the accuracy of the predicted results.

2.6 CCAI-based enrichment analysis in OC

The R packages "enrichplot", "DOSE", "limma", "org.Hs.eg.db" and "clusterProfiler" were used to perform GSEA to identify functions and pathways enriched in high- and low-risk populations [21]. Subsequently, the "limma" package was performed to identify DEGs (Fold Change > 2, FDR < 0.05) between the two stratified populations. Gene Ontology (GO) analysis and KEGG enrichment analysis were then performed on these DEGs. Furthermore, Spearman correlation analysis was used to explore the relationships between CCAI-related genes and key KEGG signaling pathways, with visualization performed using the "limma", "GSVA", "GSEABase", "reshape2" and "ggplot2" packages.

2.7 CCAI-based TIME analysis in OC

The TIMER platform estimates the degree of immune cells infiltration in tumours using various algorithms [19]. Based on the immune cell data matrix retrieved from the TIMER, we analysed the correlation between CCAI scores and immune cells infiltration using Spearman correlation analysis. The R packages "ggtext", "tidyverse", "ggplot2", "scales" and "ggpubr" were employed for the Spearman analysis and for creating correlation bubble plots and scatter plots. Additionally, the CIBERSORT algorithm was used to estimate the relative proportions of 22 immune cell types in the TCGA-OV set and to analyse differences in immune cell infiltration between the two risk subgroups. Furthermore, R package "ESTIMATE" was used to perform the ESTIMATE analysis to assess the level of immune and stromal cell infiltration in the tumor tissue, and to calculate immune and stromal cell scores for each sample [22]. The R package "ggpubr" was also employed to analyse the variability of these scores across different CCAI subgroups. Moreover, the "GSEABase" and "GSVA" packages were used in the single-sample GSEA (ssGSEA) algorithm to quantify immune cell infiltration, estimate immune function and immune cell scores, and analysis the variability of ssGSEA results between the different CCAI subgroups.

In the evolution of oncology research, immune checkpoints (ICs) and immune checkpoint inhibitors (ICIs) have become crucial components of anti-tumor therapy [23]. However, the efficacy of ICIs varies significantly across patients, highlighting the importance of distinguishing between different immune subgroups. In this study, we systematically analyzed the expression of ICs between two risk subgroups.

2.8 CCAI-based tumor mutation burden (TMB) analysis

By downloading the nucleotide variation data from the TCGA-OV cohort and using Perl scripts, we calculated the TMB values for each sample. Based on the median TMB value, patients were divided into high and low TMB groups. Survival differences between the high and low TMB subgroups were then analyzed using the K-M method. Additionally, TMB values were compared between the high and low CCAI score subgroups, and the expression of CCAI-related genes in these TMB subgroups was also analyzed.

2.9 CCAI-based drug sensitivity analysis

The 'pRRophetic' R package predicts tumor responses to various anticancer drugs based on gene expression levels [24]. We applied the 'pRRophetic' package to assess the correlation between CCAI scores and the IC50 values of different anticancer drugs in the TCGA-OC cohort, evaluating the potential significance of CCAI in guiding clinical drug therapy.

3 Results

3.1 Identification of CAFs in OV

The EMTAB8107 cohort includes single-cell sequencing data from tumor tissue of 5 ovarian cancer patients (Fig. 1A). Based on classical cell marker annotations, the EMTAB8107 cohort identified eight distinct cell categories (Fig. 1B, C), with CD8 T cells comprising a proportion second only to fibroblasts, malignant cells, and monocyte macrophages

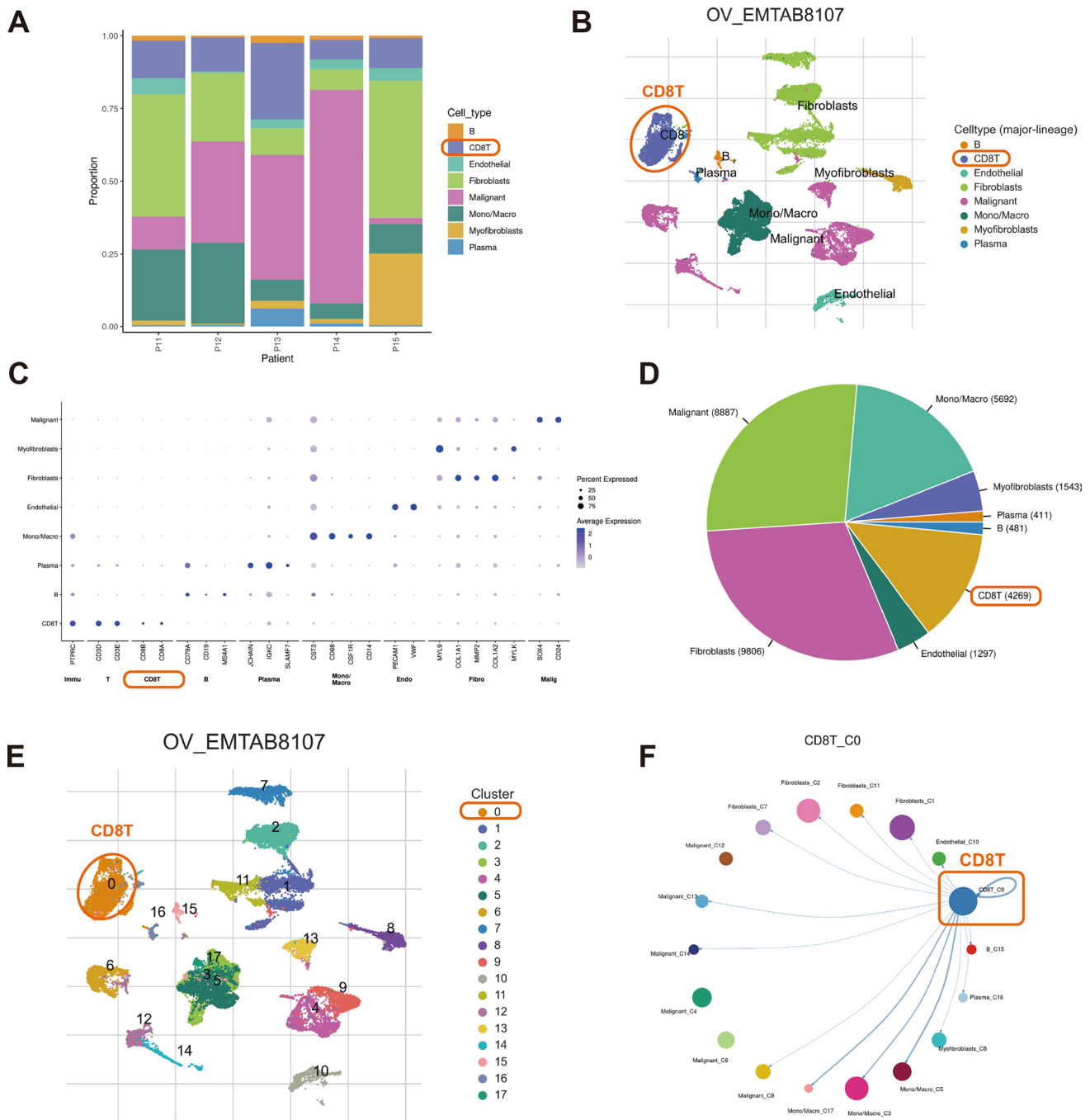

Fig. 1 Identification of CD8 T cell in OC. **A** The EMTAB8107 cohort includes single-cell sequencing data from five patients with OC. **B**, **C** The EMTAB8107 cohort identified eight cell categories based on classical cell marker annotations. **D** Pie chart showing the proportions of the eight cell types. **E** The EMTAB8107 cohort identified 17 cell clusters based on machine learning algorithm. **F** Correlation showing the relationships between CD8 T cells and other cell clusters

(Fig. 1D). Additionally, the machine learning algorithm t-distributed stochastic neighbour embedding identified 17 cell clusters, with CD8 T cells predominantly belonging to cluster 0 (Fig. 1E). The network map revealed strong connections between CD8 T cells and clusters of malignant cells, monocyte macrophages and fibroblasts (Fig. 1F).

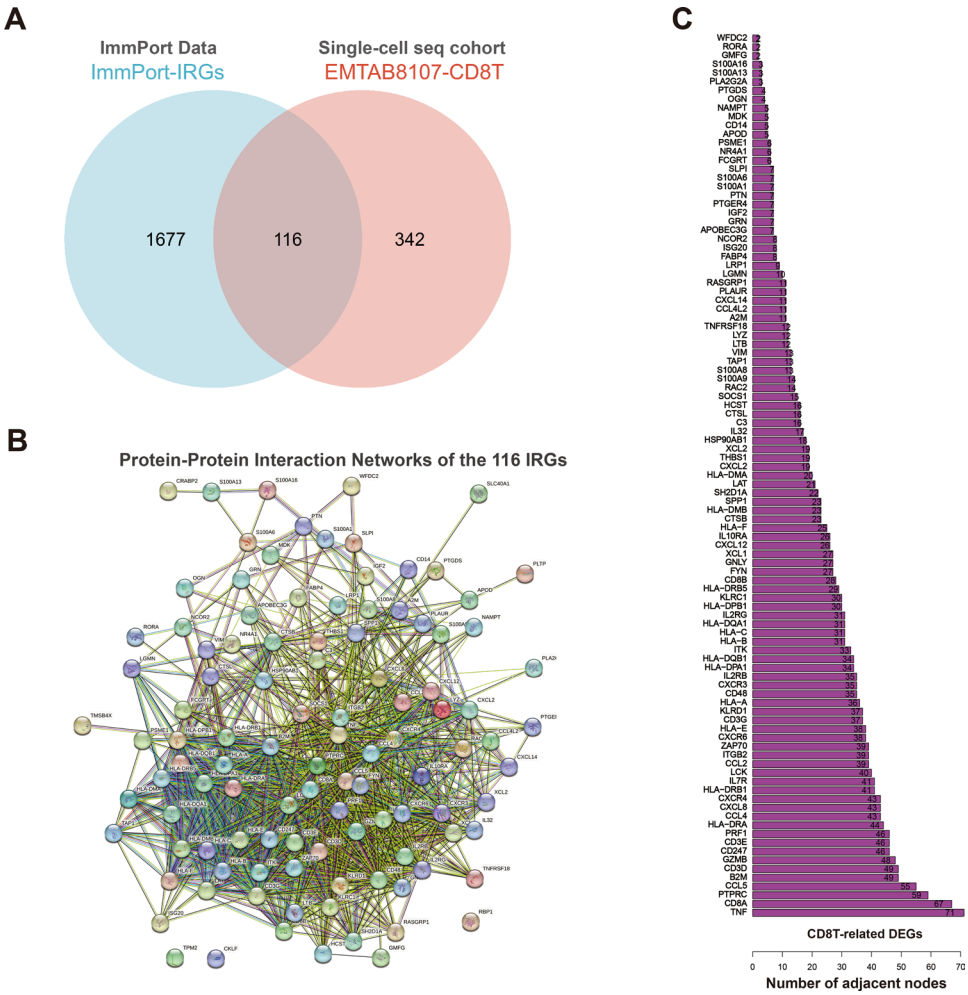

Fig. 2 CD8 T cell-associated DEGs in OC. **A** The intersection of CD8T cell-associated DEGs with IRGs from the ImmPort database identified 116 IRGs that were differentially expressed in CD8 T cells. **B** PPI analysis revealed the interactions of these 116 IRGs. **C** The eighbourhood node ordering map of these 116 genes

Table 2 Cox regression analysis of IRGs differentially expressed in CD8 T cells

Gene	Hazard ratio (HR)	HR.95L	HR.95H	*P*-value
HLA-F	0.894	0.803	0.994	0.039
TAP1	0.898	0.820	0.985	0.022
ISG20	0.845	0.754	0.946	0.004
LRP1	1.163	1.027	1.317	0.017
CXCR4	0.883	0.793	0.984	0.025
IGKC	0.962	0.927	0.997	0.035
PLAUR	1.141	1.005	1.295	0.041
OGN	1.114	1.028	1.207	0.008
IL2RG	0.869	0.789	0.956	0.004
LCK	0.864	0.755	0.989	0.034
SH2D1A	0.769	0.608	0.973	0.028
GZMB	0.892	0.811	0.982	0.020
CD3D	0.885	0.805	0.974	0.012
CD3E	0.905	0.820	0.998	0.046
CD3G	0.768	0.640	0.920	0.004
TRAC	0.911	0.839	0.989	0.026
TRBC1	0.907	0.840	0.979	0.013

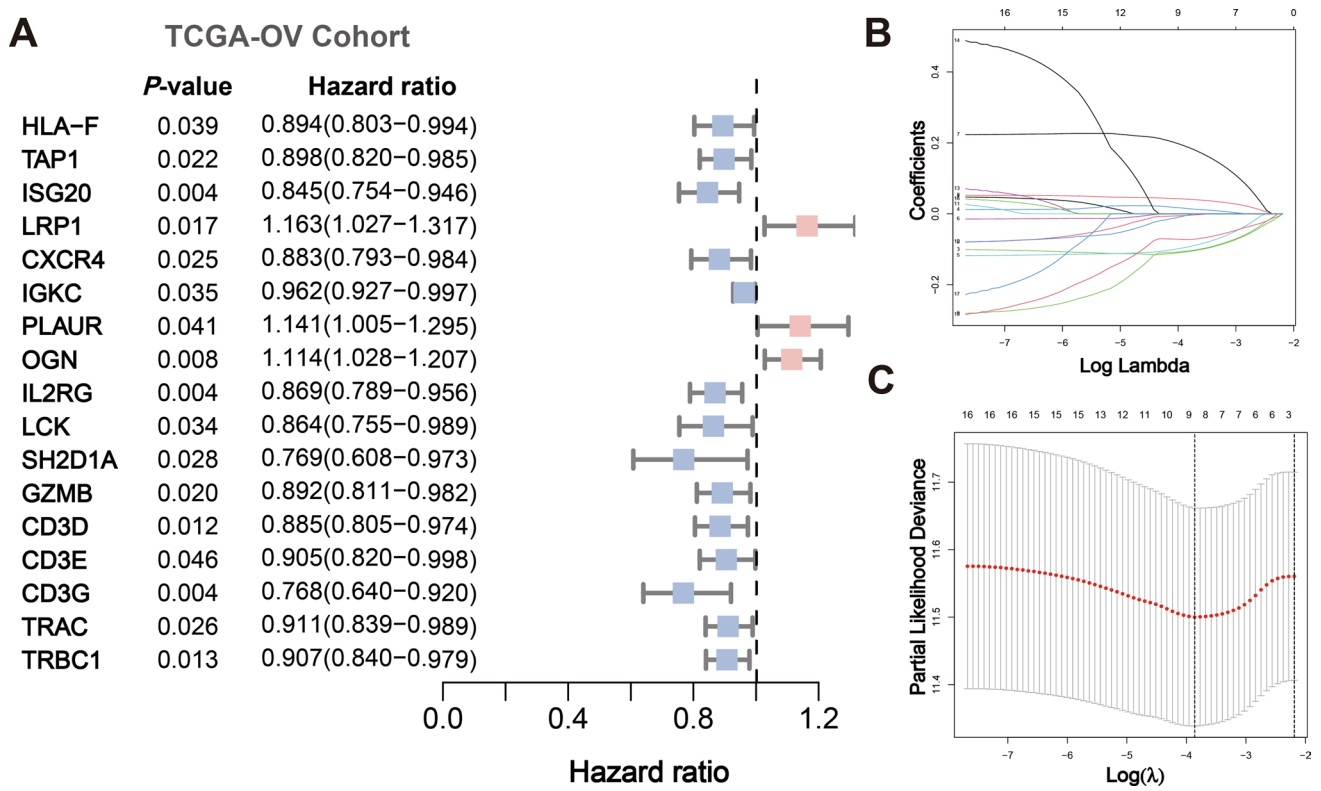

Fig. 3 Construction of the CCAI in OC**. A** Univariate Cox identified 17 IRGs significantly associated with disease HR in OC patients. **B**, **C** LASSO regression identifies genes for constructing the CCAI

Table 3 CD8T cell-related index for ovarian cancer

Index factor	Coefficient	Association with outcome
TAP1	−0.004648235	Associated with better outcome
ISG20	−0.107240807	Associated with better outcome
LRP1	0.015253703	Associated with poorer outcome
CXCR4	−0.094351506	Associated with better outcome
PLAUR	0.189890158	Associated with poorer outcome
OGN	0.041441964	Associated with poorer outcome
IL2RG	−0.10531695	Associated with better outcome
LCK	−0.004777555	Associated with better outcome
CD3G	−0.072098181	Associated with better outcome

3.2 CD8 T cell-associated DEGs in OC

We identified 458 genes that were differentially expressed between CD8 T cells and other cell types. These genes were intersected with the ImmPort database of immune-related genes (IRGs), resulting in 116 immune-associated DEGs (Fig. 2A). These 116 genes were identified as IRGs differentially expressed in CD8 T cells. Protein–protein interaction (PPI) analysis revealed the interactions of these 116 IRGs (Fig. 2B), and the neighbourhood node ordering map of these genes is shown in Fig. 2C.

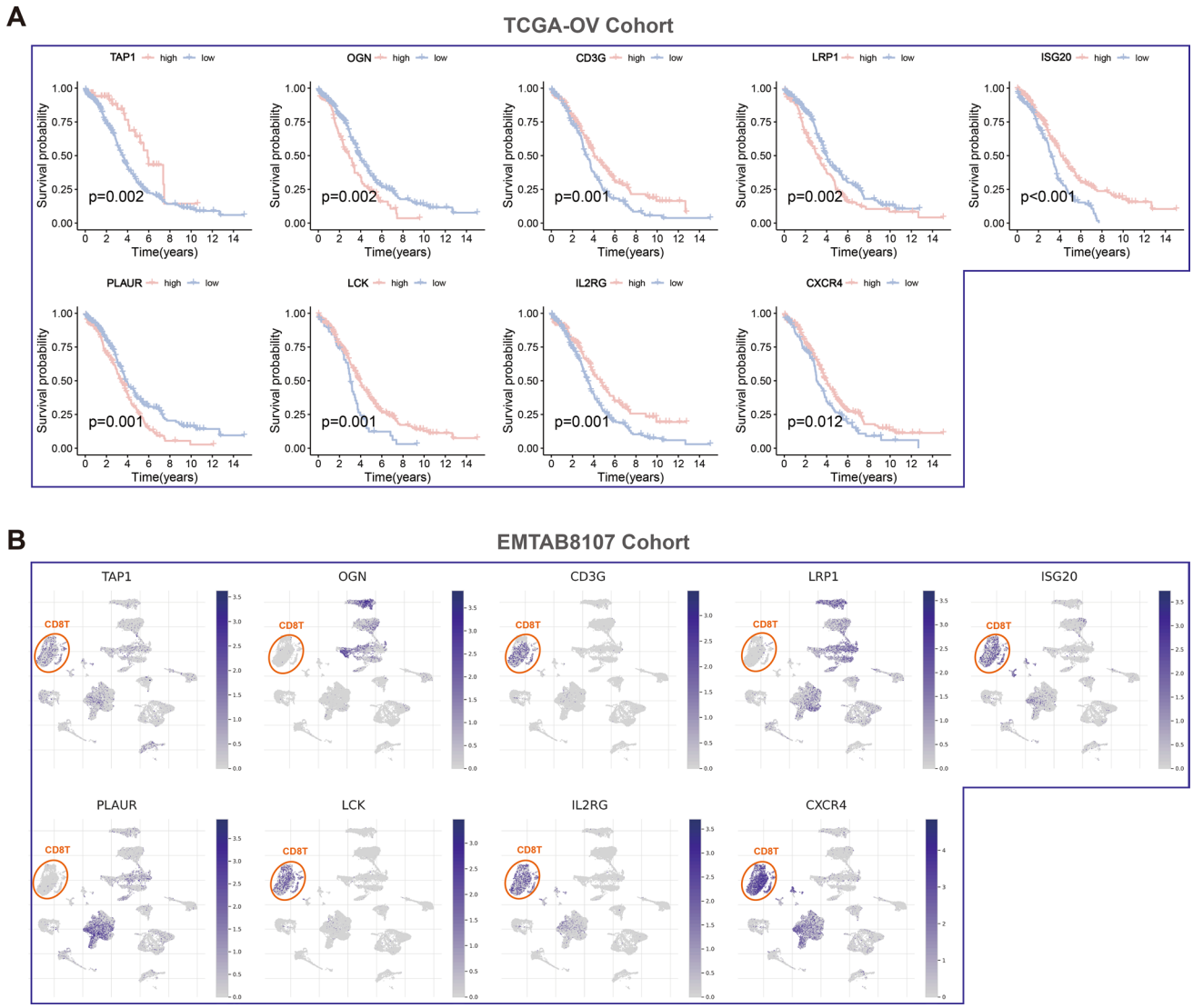

Fig. 4 CCAI-associated genes in OC**. A** K-M survival curves for the nine CCAI-associated genes in the TCGA-OV cohort. **B** Expression of the nine CCAI-related genes in CD8 T cells of the EMTAB8107 cohort

3.3 Construction of the CCAI

The univariate Cox regression for 166 IRGs differentially expressed in CD8 T cells identified 17 IRGs significantly associated with the disease Hazard Ratio (HR) in OC patients ($P < 0.05$) (Table 2), including 3 genes associated with poorer outcomes and 14 genes associated with better outcomes (Fig. 3A). Subsequently, we performed LASSO regression analyses (Fig. 3B,C) to optimize model fitting and ensure the constructed CCAI had good generalizability. Finally, LASSO identified 9 IRGs for CCAI construction (Table 3). Based on the LASSO regression coefficients and the expression values of the IRGs, the CCAI score for each patient was calculatedas follows: CCAI (score) = LRP1*(0.015253703) + PLAUR*0.189890158) + OGN*(0.041441964) − TAP1*(0.004648235) − ISG20*(0.107240807) − CXCR4*(0.094351506) − IL2RG*(0.10531695) − LCK*(0.004777555) − CD3G*(0.072098181).

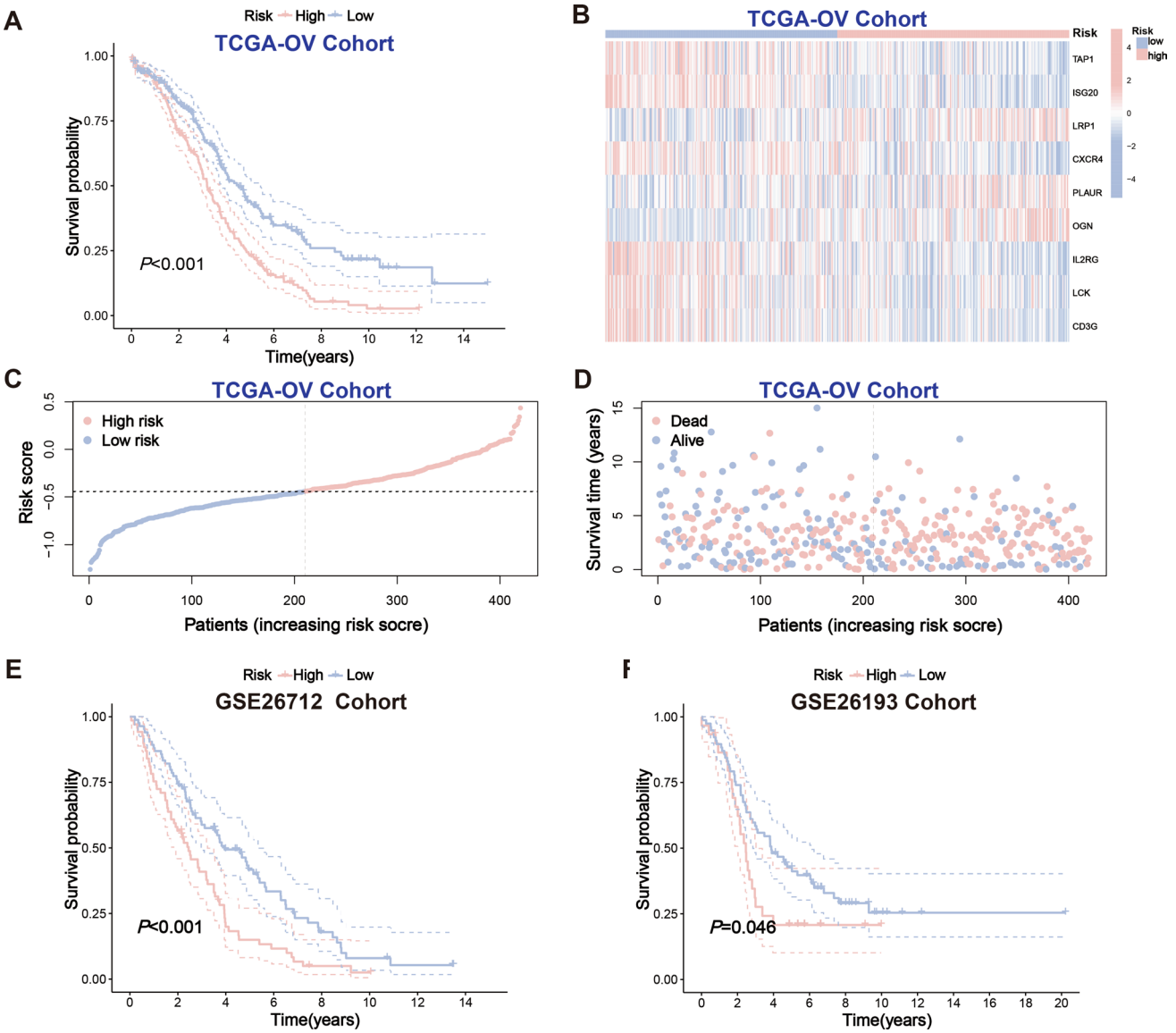

Fig. 5 Verification of CCAI**. A** K-M survival curves based on CCAI in the training set. **B** Expression of CCAI-related genes in the training cohort. **C**–**D** Distribution of ranked CCAI scores and survival status in the training cohort. **E**–**F** K-M survival curves based on CCAI in the two validation cohorts

3.4 CCAI-related genes in OC

K-M analysis showed that high expression of TAP1, ISG20, CXCR4, IL2RG, LCK and CD3G in the CCAI was associated with better prognosis in OC, whereas high expression of LRP1, PLAUR and OGN was associated with poorer prognosis (Fig. 4A). Furthermore, Fig. 4B shows the expression of the nine CCAI-related genes in CD8 T cells of the EMTAB8107 cohort. The combined expression violin plot indicated that CXCR4, IL2RG and LCK were highly expressed in CD8 T cells, while LRP1, PLAUR and OGN were expressed at lower levels in these cells (Figure S1). Figure S2A-G presents the immunohistochemical images of CCAI-related genes in OC tumor tissues from the HPA database.

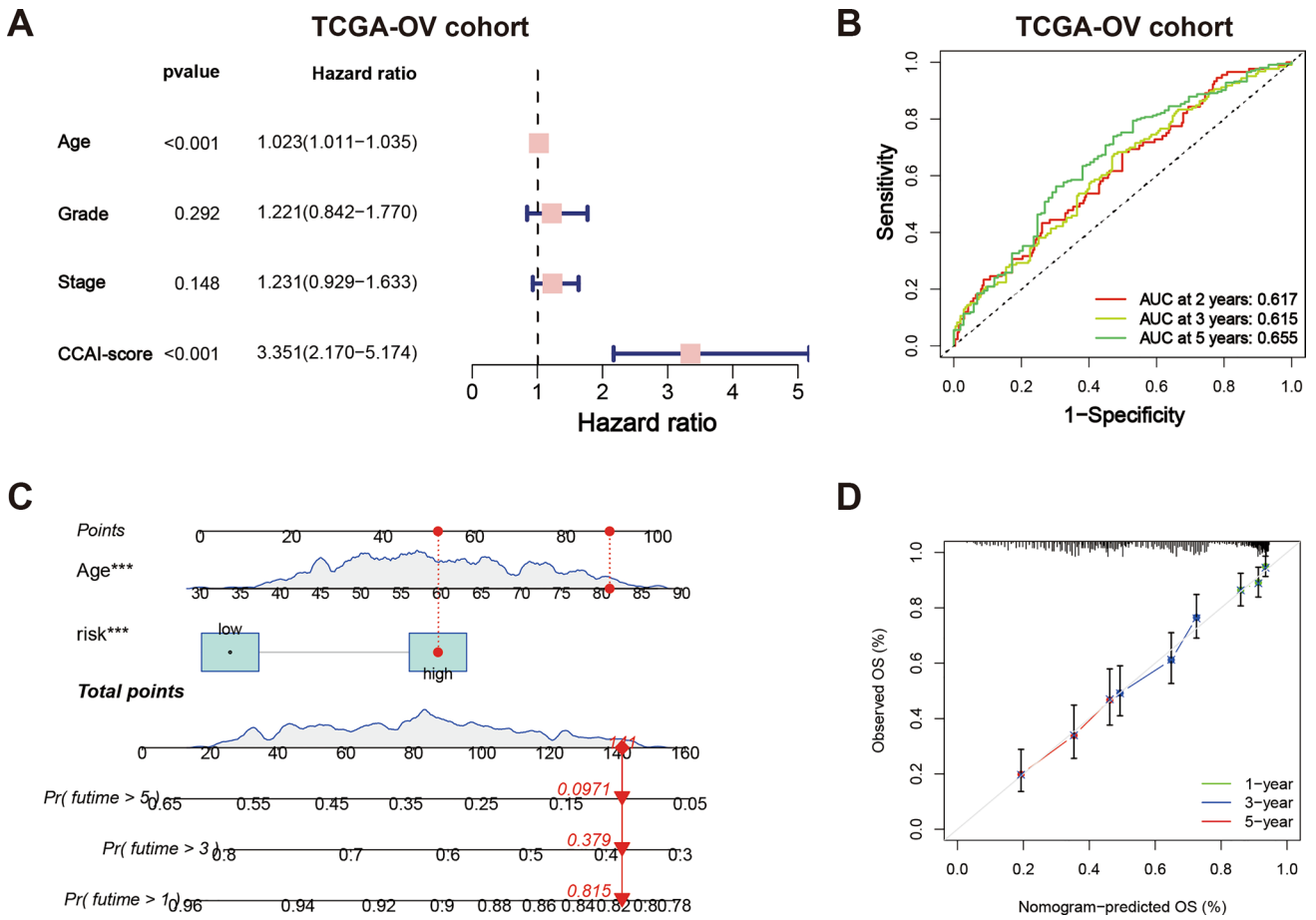

Fig. 6 Evaluation of CCAI and CCAI-based nomogram. **A** Multivariate Cox of CCAI scores and clinical parameters. **B** ROC curves for CCAI at 2, 3, and 5 years. **C** Nomogram for predicting survival in OC patients based on CCAI score and age. **D** Calibration curves for the nomogram

3.5 Verification of the validity of CCAI in predicting OC prognosis

K-M analysis demonstrated that patients in the low-CCAI group had significantly better survival compared to those in the high-CCAI group based on the CCAI score in the training set ($P < 0.001$) (Fig. 5A). Additionally, the heatmap revealed that LRP1, PLAUR, and OGN were highly expressed in the high-CCAI group, while the remaining six CCAI-related genes exhibited lower expression (Fig. 5B). Moreover, the proportion of patients who experienced mortality increased with higher CCAI scores (Fig. 5C, D). Further validation in independent cohorts showed that the survival rates of low-CCAI individuals in the GSE26712 ($P < 0.001$) and GSE26193 ($P = 0.046$) cohorts were also significantly better than those in the high-CCAI subgroup (Fig. 5E, F), further confirming the prognostic utility of CCAI in ovarian cancer.

3.6 Evaluation of CCAI in OC

Multivariate Cox regression analysis of CCAI scores and clinical parameters indicated that CCAI scores were an independent prognostic factor for OC, with an HR value of 3.351 ($P < 0.001$) (Fig. 6A). Additionally, age was also identified as an independent prognostic factor for OC, with an HR value of 1.023 ($P < 0.001$). Furthermore, ROC analysis r showed that the AUC values for CCAI at 2, 3, and 5 years were 0.617, 0.615, and 0.655, respectively (Fig. 6B).

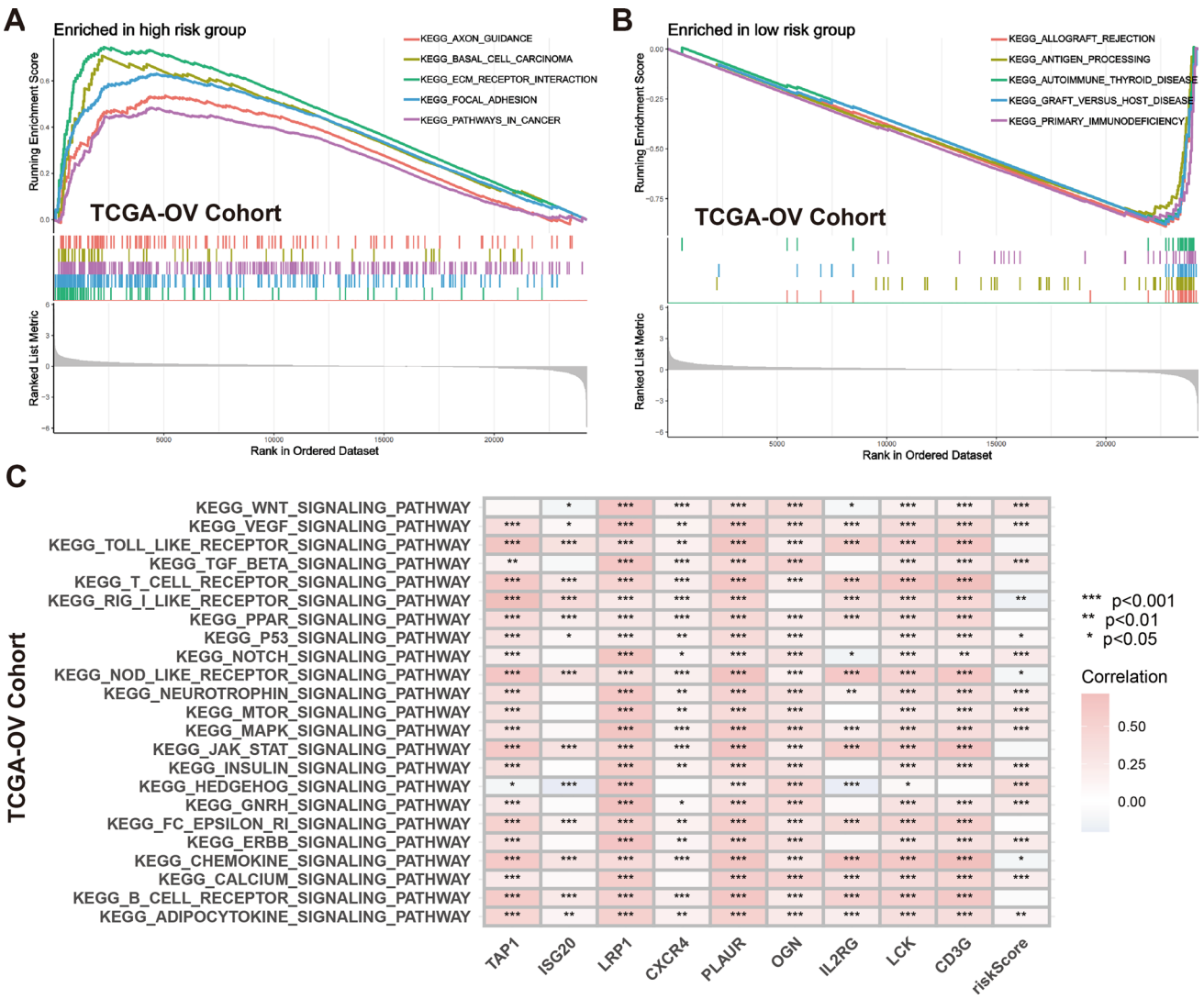

Fig. 7 GSEA for CCAI-based stratification**. A** GSEA showing enriched functions and pathways in the high CCAI groups. **B** GSEA showing enriched functions and pathways in the low CCAI groups **C** Heatmap showing the association between the expression of CCAI-related moleculars and key signaling pathways

3.7 CCAI-based nomograms for predicting OC prognosis

We constructed a nomogram to predict survival in OC patients based on CCAI score and age. The nomogram estimated 1-, 3- and 5-year survival rates to be 0.815, 0.379 and 0.0971, respectively, for an 81-year-old high-risk OC patient (Fig. 6C). Additionally, calibration curves showed that the nomogram's predictions aligned excellently with the actual survival rates (Fig. 6D).

3.8 GSEA, GO and KEGG analyses for CCAI-based stratification

GSEA results revealed that the axon guidance, extracellular matrix-receptor interaction signalling pathways, focal adhesion and pathways in cancer were enriched in the high CCAI group (Fig. 7A). In contrast, antigen processing and presentation, primary immunodeficiency, and allograft rejection were enriched in the low CCAI subgroup (Fig. 7B). Additionally, the expression of CCAI-associated genes was significantly correlated with the status of key signaling pathways (Fig. 7C).

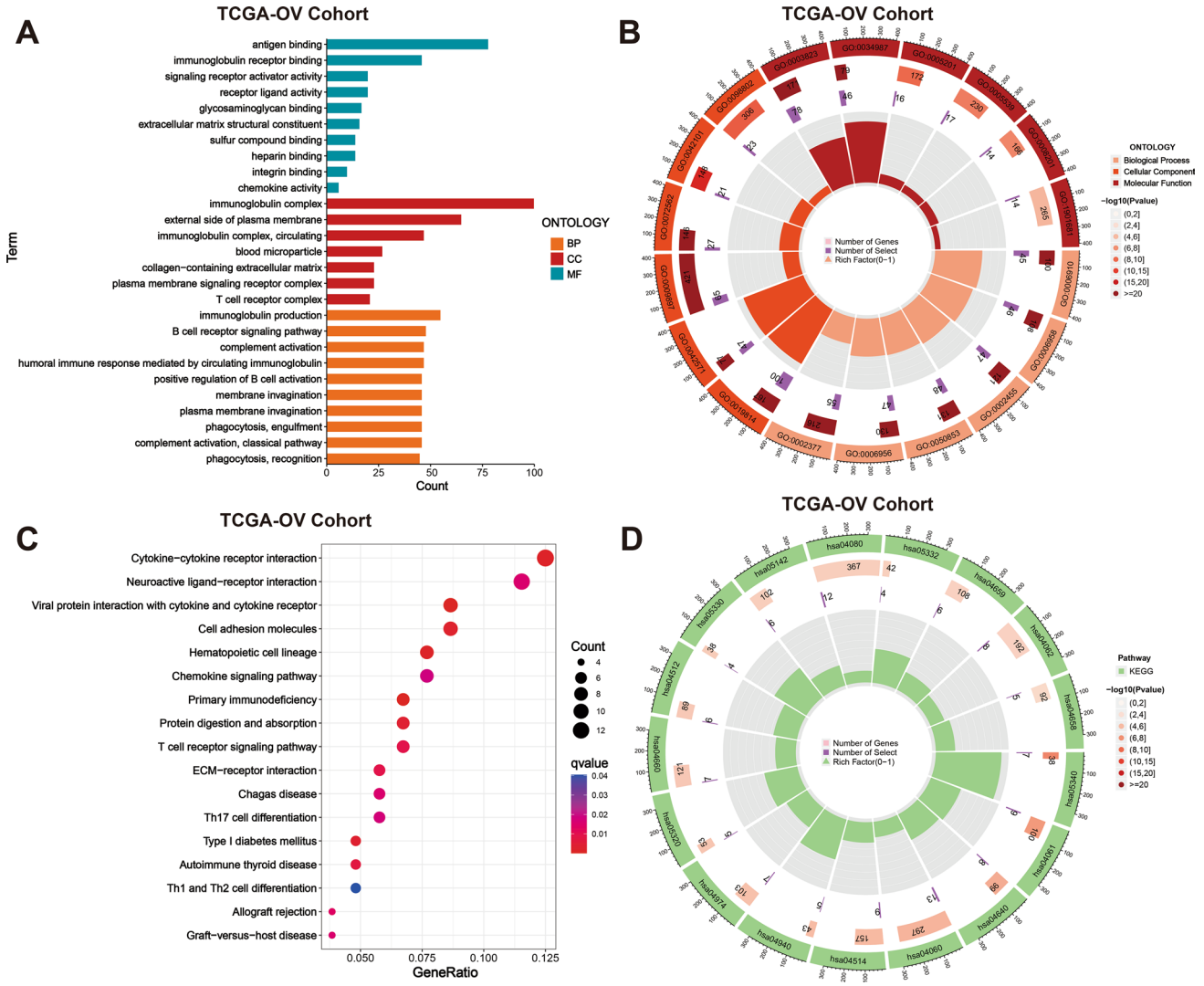

Fig. 8 GO and KEGG analyses for CCAI-based stratification. **A**, **B** GO analysis of DEGs between high and low CCAI subgroups. **C**, **D** KEGG analysis of DEGs between high and low CCAI subgroups

We further identified the DEGs between the high and low CCAI subgroups. GO analysis showed that these DEGs were enriched in antigen binding, immunoglobulin receiver binding, signaling receiver activation activity, immunoglobulin complex, external side of plasma membrane, immunoglobulin complex circulating, T cell receiver complex, immunoglobulin production, and B cell receiver signaling pathway (Fig. 8A, B). Additionally, KEGG analysis revealed that the DEGs were enriched in cytokine-cytokine receptor interaction, neuroactive ligand-receptor interaction, T cell receptor signaling pathway and primary immunodeficiency pathways (Fig. 8C, D).

3.9 CCAI characterises the immune microenvironment of OC

TIMER analysis demonstrated that the CCAI score was inversely correlated with the degree of infiltration of most immune cells in OC tumor tissues (Fig. 9A). Scatter plots showing the correlation between CCAI score and the infiltration levels of CD8+ T cells are presented in Fig. 9B. CIBERSORT algorithm validation indicated that the infiltration of CD8 T cells, Tregs cells and M1 macrophages was significantly lower in the high CCAI group, whereas M2 macrophages presented a higher level of infiltration in the high CCAI group (Fig. 10A). Additionally, ESTIMATE algorithm analysis revealed that the immunity score was significantly higher in the low CCAI subgroup, while the stromal score showed the opposite situation (Fig. 10B, C). Further validation using the ssGSEA algorithm validation showed that most of the immune cell infiltration and immune functions were significantly stronger in the low CCAI group (Fig. 10D, E).

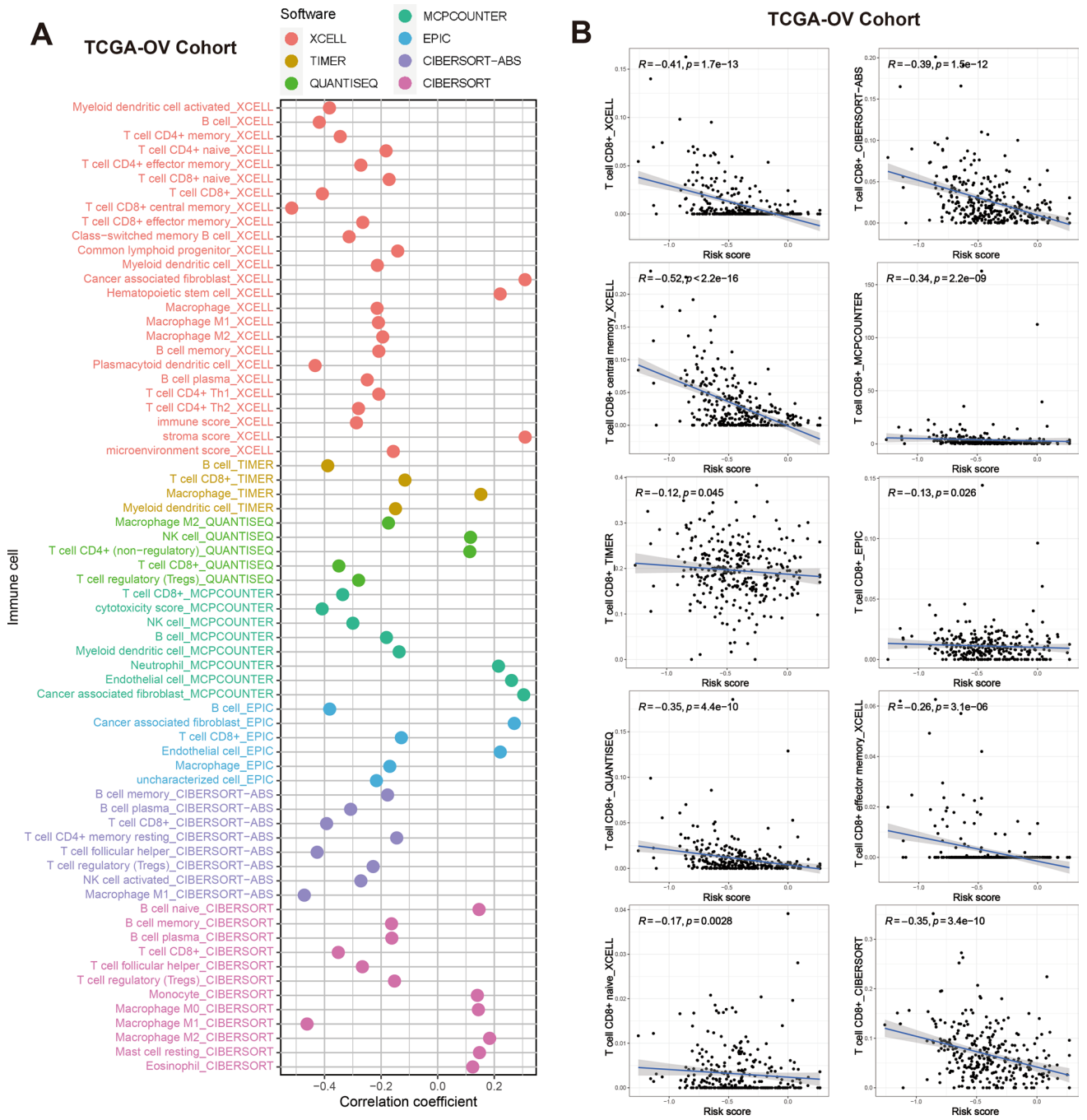

Fig. 9 Correlation of CCAI scores with immune cells. **A** Correlation between CCAI scores and immune cells assessed by various algorithms on the TIMER platform. **B** Scatter plots showing the relationship between CCAI score and the infiltration levels of CD8 T cells

The immune infiltration status of the tumor and the activation status of ICs are key determinants of the tumor's response to ICIs [23]. Analysis of ICs revealed that most ICs were expressed at higher levels in the low CCAI subgroup (Fig. 10F).

3.10 CCAI-based TMB and drug sensitivity analysis

K-M analysis revealed that patients in the high TMB group had better survival outcomes compared to those in the low TMB group (Figure S3A). However, no significant difference in TMB was observed between the high and low

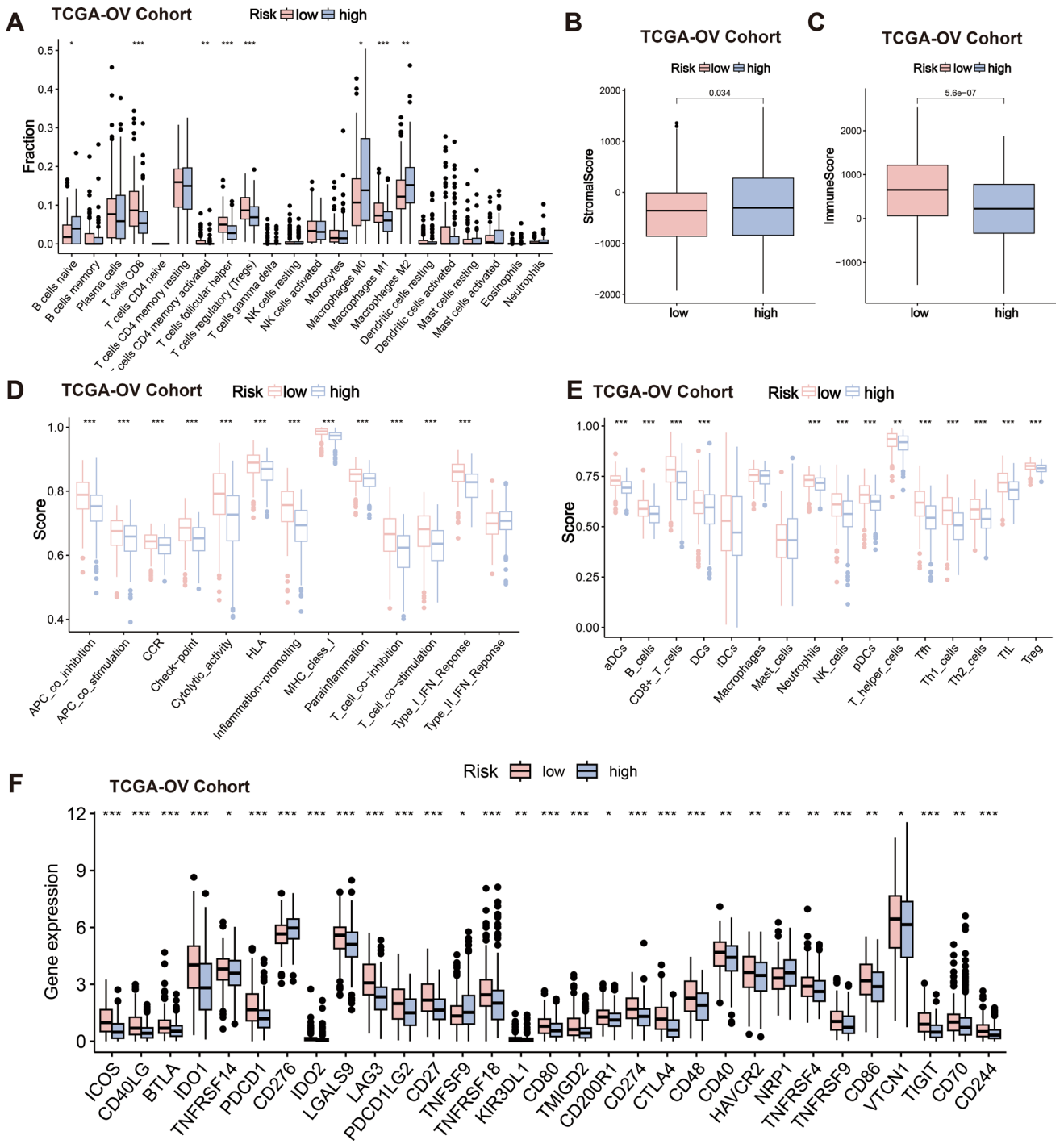

Fig. 10 Validation of CIBERSORT, ESTIMATE and ssGSEA algorithms**. A** CIBERSORT verifies the relationship between CCAI scores and the immune microenvironment. **B**, **C** ESTIMATE algorithm assesses CCAI score in relation to immune score and stroma score. **D** ssGSEA verifies the correlation between CCAI score and immune function. **E** ssGSEA verifies the correlation between CCAI score and immune cells

CCAI subgroups (Figure S3B). Additionally, we found that LRP1 was underexpressed in the high TMB group, whereas ISG20 was overexpressed in the high TMB group (Figure S3C). Nevertheless, the majority of CCAI gene expressions did not show significant differences between high and low TMB groups. Additionally, the correlation scatter plots show that CCAI scores were significantly correlated with the IC50 values of drugs such as axitinib, erlotinib, sorafenib, and docetaxel (Figure S4).

4 Discussion

The immune cell play a crucial role in the tumor microenvironment, where intercellular communication, primarily mediated by ligand-receptor interactions, significantly influences tumor metastasis, drug resistance, and response to chemotherapy [25, 26]. Previous studies have highlighted the correlation between CD8 T cell infiltration and immunotherapy outcomes [27–29]. Additionally, several immunotherapy targets have been identified within CD8 T cells [30], underscoring their potential relevance for various anti-cancer treatments. Furthermore, researches have established the association between tumor-infiltrating immune cells and clinical outcomes in OC [31–33]. Therefore, understanding the distinct role of CD8 T cells in evaluating clinical outcomes and immune landscape in OC will contribute to the identification of efficient predictive biomarkers. In this study, we aim to elucidate the significance of markers associated with CD8 T cell infiltration in patients with OC.

In the present work, we developed a CCAI composed of nine IRGs to predict the prognosis and characterising TIME features of OC patients, using high-throughput sequencing data and machine learning algorithms analysis. Both Cox and ROC analyses demonstrated that CCAI is a potential prognostic predictor for OC and serves as an independent survival indicator with good stability. The predictive validity of CCAI was further validated in two independent OC cohorts. The combined validation and evaluation results suggest that CCAI could serve as a potentially effective prognostic biomarker for OC.

Among the nine IRGs that make up the CCAI, LRP1, PLAUR and OGN are associated with poorer outcomes in OC, and notably all three are lowly expressed in CD8T cells. Among them, OGN has been suggested to be a possible pivotal gene in polycystic ovary syndrome (PCOS) and ovarian cancer progression, which regulating hormonal responses in both PCOS and OC [34]. In addition, OGN has been demonstrated to be associated with EMT characteristics and poor prognosis in OC [35]. The miR-1290/OGN axis in OC-associated fibroblasts has been shown to regulate tumor cell evolution [36]. In a previous study, LRP1 in serum exosomes of OC patients contributed to the migration of tumor cells and has been suggested as a potential biomarker [37]. Although PLAUR has been reported to play a key role in ovarian function [38], its exact contribution to OC remains unclear. Therefore, the mechanism of the role of CCAI-related molecules in OC warrants further investigation in subsequent studies.

Despite the high initial treatment efficacy of OC, patients unfortunately remain at an extremely high risk of disease recurrence after first-line treatment. Therefore, there is a pressing need to discover treatment modalities that are both effective and safe, offering not only favourable therapeutic responses but also reduced toxicity and fewer side effects. In recent years, immunotherapy, particularly ICIs, has gradually become a efficient strategy for clinical treatment and has taken a leading role in the systemic treatment of many cancers [39–41]. ICIs activate and promote the proliferation of tumor effector T cells and specifically target immunosuppressive cells in TIME to restore the immune system's ability to recognize and eliminate tumor cells [42]. However, in clinical practice, the response rate of ICIs remains suboptimal, with only some patients can benefit from ICIs treatment. While clinical studies of ICIs have been conducted in selected OC cohorts, their clinical application has been hindered by a lack of sufficient evidence-based medical data [42–44]. Therefore, understanding and characterising tumor subpopulations with different TIME characteristics will help to better explore the key biological mechanisms and ultimately identify patient populations that are more likely to benefit of immunotherapy.

The CIBERSORT, TIMER, ESTIMATE and ssGSEA algorithm analyses in this study collectively indicated that tumour-infiltrating CD8 T cells were higher in the low CCAI population. Additionally, most ICs also showed higher levels of expression in the low CCAI population. Notably, previous studies have defined tumours characterised by high levels of CD8 T cell infiltration and overexpression of ICs as immunoinflammatory tumours [45, 46], which have been shown to achieve better disease remission when treated with ICIs [47]. These results suggest that the low CCAI subpopulation is more likely to be immunoinflammatory, potentially leading to a better response rate to ICIs compared to the high CCAI population.

Although independent cohorts from different databases were included in this study for comprehensive analyses and assessment, there are limitations. Firstly, in the retrospective analysis of the study, we were unable to assess the potential bias of the included data. Secondly, the study lacks prospective data to further evaluate the role of CCAI in predicting prognosis and response to immunotherapy. Notably, the conclusions drawn regarding the predictive value of CCAI for ICIs response have not been validated in ovarian cancer cohorts treated with ICIs. The absence of such validation means that the potential of CCAI as a predictive biomarker for immunotherapy efficacy in OC needs further confirmation. Future clinical studies should focus on collecting prospective ICI treatment data from OC cohorts to refine the role of CCAI and validate its clinical utility as a prognostic and predictive biomarker.

5 Conclusion

In this work, the CCAI was developed to predict the clinical outcomes of OC. The CCAI score was significantly correlated with OC survival and could independently predict prognosis with good accuracy and stability. Additionally, the CCAI score correlated with TIME of OC and may have potential in predicting the immune landscape. This study provides valuable insights into the mechanism by which CD8T cell-associated IRGs influence OC prognosis.

Author contributions Yu Zhang designed the study, supervised the research, and drafted the manuscript. Peng Wan and Liangliang Wang performed the analysis. Ruiping Ren analyzed the information and took part in the manuscript revisions. All authors reviewed the final draft and approved its submission.

Funding This work was funded by the Project of NINGBO Leading Medical & Health Discipline, Project Number: 2022-X07.

Data availability The datasets used and analysed during this study available from the corresponding author on reasonable request.

Declarations

Competing interests The authors declare no competing interests.

References

1. Sung H, Ferlay J, Siegel RL, Laversanne M, Soerjomataram I, Jemal A, Bray F. Global Cancer Statistics 2020: GLOBOCAN estimates of incidence and mortality worldwide for 36 cancers in 185 countries. CA Cancer J Clin. 2021;71(3):209–49.
2. Stewart C, Ralyea C, Lockwood S. Ovarian cancer: an integrated review. Semin Oncol Nurs. 2019;35(2):151–6.
3. Colombo N, Sessa C, du Bois A, Ledermann J, McCluggage WG, McNeish I, Morice P, Pignata S, Ray-Coquard I, Vergote I, Baert T, Belaroussi I, Dashora A, et al. ESMO-ESGO consensus conference recommendations on ovarian cancer: pathology and molecular biology, early and advanced stages, borderline tumours and recurrent disease. Ann Oncol. 2019;30(5):672–705.
4. Eisenhauer EA. Real-world evidence in the treatment of ovarian cancer. Ann Oncol. 2017;28(suppl_8):viii61–5.
5. Zhang L, Conejo-Garcia JR, Katsaros D, Gimotty PA, Massobrio M, Regnani G, Makrigiannakis A, Gray H, Schlienger K, Liebman MN, Rubin SC, Coukos G. Intratumoral T cells, recurrence, and survival in epithelial ovarian cancer. N Engl J Med. 2003;348(3):203–13.
6. Li J, Wang J, Chen R, Bai Y, Lu X. The prognostic value of tumor-infiltrating T lymphocytes in ovarian cancer. Oncotarget. 2017;8(9):15621–31.
7. Tubridy EA, Eiva MA, Liu F, Omran DK, Gysler S, Brown EG, Roy AG, Zeng Y, Oh J, Cao Q, Gitto SB, Powell DJ Jr. CD137+ tumor infiltrating lymphocytes predicts ovarian cancer survival. Gynecol Oncol. 2024;184:74–82.
8. Zhang W, Zhang R, Chang Z, Wang X. Resveratrol activates CD8(+) T cells through IL-18 bystander activation in lung adenocarcinoma. Front Pharmacol. 2022;13:1031438.
9. Vidal M, Fraga M, Llerena F, Vera A, Hernández M, Koch E, Reyes-López F, Vallejos-Vidal E, Cabrera-Vives G, Nova-Lamperti E. Analysis of tumor-infiltrating T-cell transcriptomes reveal a unique genetic signature across different types of cancer. Int J Mol Sci. 2022;23(19):11065.
10. MacNabb BW, Tumuluru S, Chen X, Godfrey J, Kasal DN, Yu J, Jongsma MLM, Spaapen RM, Kline DE, Kline J. Dendritic cells can prime anti-tumor CD8(+) T cell responses through major histocompatibility complex cross-dressing. Immunity. 2022;55(6):982-997.e988.
11. Haring JS, Badovinac VP, Harty JT. Inflaming the CD8+ T cell response. Immunity. 2006;25(1):19–29.
12. Sato E, Olson SH, Ahn J, Bundy B, Nishikawa H, Qian F, Jungbluth AA, Frosina D, Gnjatic S, Ambrosone C, Kepner J, Odunsi T, Ritter G, et al. Intraepithelial CD8+ tumor-infiltrating lymphocytes and a high CD8+/regulatory T cell ratio are associated with favorable prognosis in ovarian cancer. Proc Natl Acad Sci USA. 2005;102(51):18538–43.
13. Chen R, Zheng Y, Fei C, Ye J, Fei H. Machine learning developed a CD8(+) exhausted T cells signature for predicting prognosis, immune infiltration and drug sensitivity in ovarian cancer. Sci Rep. 2024;14(1):5794.
14. Ye Y, Zhang S, Jiang Y, Huang Y, Wang G, Zhang M, Gui Z, Wu Y, Bian G, Li P, Zhang M. Identification of a cancer associated fibroblasts-related index to predict prognosis and immune landscape in ovarian cancer. Sci Rep. 2023;13(1):21565.
15. Bao L, Wu Y, Ren Z, Huang Y, Jiang Y, Li K, Xu X, Ye Y, Gui Z. Comprehensive pan-cancer analysis indicates UCHL5 as a novel cancer biomarker and promotes cervical cancer progression through the Wnt signaling pathway. Biol Direct. 2024;19(1):139.
16. Chen R, Yao Z, Jiang L, Hu J. A Golgi apparatus-related subtype and risk signature predicts prognosis and evaluates immunotherapy response in gastric cancer. Discover Oncol. 2025;16(1):76.

17. Han Y, Wang Y, Dong X, Sun D, Liu Z, Yue J, Wang H, Li T, Wang C. TISCH2: expanded datasets and new tools for single-cell transcriptome analyses of the tumor microenvironment. Nucleic Acids Res. 2023;51(D1):D1425-d1431.
18. Pontén F, Schwenk JM, Asplund A, Edqvist PH. The Human Protein Atlas as a proteomic resource for biomarker discovery. J Intern Med. 2011;270(5):428–46.
19. Li T, Fan J, Wang B, Traugh N, Chen Q, Liu JS, Li B, Liu XS. TIMER: a web server for comprehensive analysis of tumor-infiltrating immune cells. Can Res. 2017;77(21):e108–10.
20. Bhattacharya S, Andorf S, Gomes L, Dunn P, Schaefer H, Pontius J, Berger P, Desborough V, Smith T, Campbell J, Thomson E, Monteiro R, Guimaraes P, et al. ImmPort: disseminating data to the public for the future of immunology. Immunol Res. 2014;58(2–3):234–9.
21. Subramanian A, Tamayo P, Mootha VK, Mukherjee S, Ebert BL, Gillette MA, Paulovich A, Pomeroy SL, Golub TR, Lander ES, Mesirov JP. Gene set enrichment analysis: a knowledge-based approach for interpreting genome-wide expression profiles. Proc Natl Acad Sci USA. 2005;102(43):15545–50.
22. Yoshihara K, Shahmoradgoli M, Martínez E, Vegesna R, Kim H, Torres-Garcia W, Treviño V, Shen H, Laird PW, Levine DA, Carter SL, Getz G, Stemke-Hale K, et al. Inferring tumour purity and stromal and immune cell admixture from expression data. Nat Commun. 2013;4:2612.
23. Ouyang P, Wang L, Wu J, Tian Y, Chen C, Li D, Yao Z, Chen R, Xiang G, Gong J, Bao Z. Overcoming cold tumors: a combination strategy of immune checkpoint inhibitors. Front Immunol. 2024;15:1344272.
24. Geeleher P, Cox N, Huang RS. pRRophetic: an R package for prediction of clinical chemotherapeutic response from tumor gene expression levels. PLoS ONE. 2014;9(9): e107468.
25. Khalaf K, Hana D, Chou JT, Singh C, Mackiewicz A, Kaczmarek M. Aspects of the tumor microenvironment involved in immune resistance and drug resistance. Front Immunol. 2021;12: 656364.
26. Kumar MP, Du J, Lagoudas G, Jiao Y, Sawyer A, Drummond DC, Lauffenburger DA, Raue A. Analysis of single-cell RNA-Seq identifies cell-cell communication associated with tumor characteristics. Cell Rep. 2018;25(6):1458-1468.e1454.
27. Tian Y, Wei Y, Liu H, Shang H, Xu Y, Wu T, Liu W, Huang A, Dang Q, Sun Y. Significance of CD8(+) T cell infiltration-related biomarkers and the corresponding prediction model for the prognosis of kidney renal clear cell carcinoma. Aging. 2021;13(19):22912–33.
28. Feng M, Wu Z, Zhou Y, Wei Z, Tian E, Mei S, Zhu Y, Liu C, He F, Li H, Xie C, Jin J, Dong J, et al. BCL9 regulates CD226 and CD96 checkpoints in CD8(+) T cells to improve PD-1 response in cancer. Signal Transduct Target Ther. 2021;6(1):313.
29. Kerepesi C, Abushukair HM, Ricciuti B, Nassar AH, Adib E, Alessi JV, Pecci F, Rakaee M, Fadlullah MZH, Tőkés AM, Rodig SJ, Awad MM, Tan AC, et al. Association of baseline tumor-specific neoantigens and CD8(+) T-cell infiltration with immune-related adverse events secondary to immune checkpoint inhibitors. JCO Precis Oncol. 2024;8: e2300439.
30. Dong MB, Wang G, Chow RD, Ye L, Zhu L, Dai X, Park JJ, Kim HR, Errami Y, Guzman CD, Zhou X, Chen KY, Renauer PA, et al. Systematic immunotherapy target discovery using genome-scale in vivo CRISPR screens in CD8 T Cells. Cell. 2019;178(5):1189-1204.e1123.
31. Guo N, Yang A, Farooq FB, Kalaria S, Moss E, DeVorkin L, Lesperance M, Bénard F, Wilson D, Tinker AV, Nathoo FS, Hamilton PT, Lum JJ. CD8 + T cell infiltration is associated with improved survival and negatively correlates with hypoxia in clear cell ovarian cancer. Sci Rep. 2023;13(1):6530.
32. Ölmez F, Oğlak SC, Ölmez ÖF, Akbayır Ö, Yılmaz E, Akgöl S, Konal M, Seyhan NA, Kinter AK. High expression of CD8 in the tumor microenvironment is associated with PD-1 expression and patient survival in high-grade serous ovarian cancer. Turkish J Obstet Gynecol. 2022;19(3):246–56.
33. Farrag MS, Abdelwahab K, Farrag NS, Elrefaie WE, Emarah Z. Programmed death ligand-1 and CD8 tumor-infiltrating lymphocytes (TILs) as prognostic predictors in ovarian high-grade serous carcinoma (HGSC). J Egypt Natl Canc Inst. 2021;33(1):16.
34. Zou J, Li Y, Liao N, Liu J, Zhang Q, Luo M, Xiao J, Chen Y, Wang M, Chen K, Zeng J, Mo Z. Identification of key genes associated with polycystic ovary syndrome (PCOS) and ovarian cancer using an integrated bioinformatics analysis. J Ovarian Res. 2022;15(1):30.
35. Chen H, Yang L, Sun W. Elevated OGN expression correlates with the EMT signature and poor prognosis in ovarian carcinoma. Int J Clin Exp Pathol. 2019;12(2):584–9.
36. Jiang B, Xiao S, Zhang S, Xiao F. The miR-1290/OGN axis in ovarian cancer-associated fibroblasts modulates cancer cell proliferation and invasion. J Ovarian Res. 2024;17(1):52.
37. Zhou W, Ma J, Zhao H, Wang Q, Guo X, Chen L, Cao Z, Xu J, Zhang B, Zhou X. Serum exosomes from epithelial ovarian cancer patients contain LRP1, which promotes the migration of epithelial ovarian cancer cell. Mol Cell Proteomics. 2023;22(4): 100520.
38. Zhao Y, Yu B, Liu X, Hu J, Yang Y, Namei E, Yang B, Bai Y, Qian Y, Li H. The cAMP-ERK1/2 signaling pathway regulates urokinase-type plasminogen activator-induced bovine granulosa cell proliferation. Reproduction (Cambridge, England). 2020;160(6):853–62.
39. Cai L, Chen A, Tang D. A new strategy for immunotherapy of microsatellite-stable (MSS)-type advanced colorectal cancer: multi-pathway combination therapy with PD-1/PD-L1 inhibitors. Immunology. 2024;173(2):209–26. https://doi.org/10.1111/imm.13785.
40. Parvez A, Choudhary F, Mudgal P, Khan R, Qureshi KA, Farooqi H, Aspatwar A. PD-1 and PD-L1: architects of immune symphony and immunotherapy breakthroughs in cancer treatment. Front Immunol. 2023;14:1296341.
41. VanderWalde A, Bellasea SL, Kendra KL, Khushalani NI, Campbell KM, Scumpia PO, Kuklinski LF, Collichio F, Sosman JA, Ikeguchi A, Victor AI, Truong TG, Chmielowski B, et al. Ipilimumab with or without nivolumab in PD-1 or PD-L1 blockade refractory metastatic melanoma: a randomized phase 2 trial. Nat Med. 2023;29(9):2278–85.
42. Siminiak N, Czepczyński R, Zaborowski MP, Iżycki D. Immunotherapy in ovarian cancer. Arch Immunol Ther Exp. 2022;70(1):19.
43. Hamanishi J, Mandai M, Ikeda T, Minami M, Kawaguchi A, Murayama T, Kanai M, Mori Y, Matsumoto S, Chikuma S, Matsumura N, Abiko K, Baba T, et al. Safety and antitumor activity of anti-PD-1 antibody, nivolumab, in patients with platinum-resistant ovarian cancer. J Clin Oncol. 2015;33(34):4015–22.
44. Hamanishi J, Mandai M, Konishi I. Immune checkpoint inhibition in ovarian cancer. Int Immunol. 2016;28(7):339–48.
45. Chen DS, Mellman I. Elements of cancer immunity and the cancer-immune set point. Nature. 2017;541(7637):321–30.
46. Liu YT, Sun ZJ. Turning cold tumors into hot tumors by improving T-cell infiltration. Theranostics. 2021;11(11):5365–86.
47. Galon J, Bruni D. Approaches to treat immune hot, altered and cold tumours with combination immunotherapies. Nat Rev Drug Discovery. 2019;18(3):197–218.